

# The role of the Yoshizawa effect in the Archontis dynamo

Sharanya Sur<sup>1</sup>★ and Axel Brandenburg<sup>2,3</sup>★

<sup>1</sup>*Inter-University Centre for Astronomy and Astrophysics, Post Bag 4, Ganeshkhind, Pune 411 007, India*

<sup>2</sup>*NORDITA, AlbaNova University Center, Roslagstullsbacken 23, SE 10691 Stockholm, Sweden*

<sup>3</sup>*Department of Astronomy, AlbaNova University Center, Stockholm University, SE 10691 Stockholm, Sweden*

Accepted 2009 June 15. Received 2009 April 27; in original form 2009 February 16

## ABSTRACT

The generation of mean magnetic fields is studied for a simple non-helical flow where a net cross-helicity of either sign can emerge. This flow, which is also known as the Archontis flow, is a generalization of the Arnold–Beltrami–Childress flow, but with the cosine terms omitted. The presence of cross-helicity leads to a mean-field dynamo effect that is known as the Yoshizawa effect. Direct numerical simulations of such flows demonstrate the presence of magnetic fields on scales larger than the scale of the flow. Contrary to earlier expectations, the Yoshizawa effect is found to be proportional to the mean magnetic field and can therefore lead to its exponential instead of just linear amplification for magnetic Reynolds numbers that exceed a certain critical value. Unlike  $\alpha$  effect dynamos, it is found that the Yoshizawa effect is not notably constrained by the presence of a conservation law. It is argued that this is due to the presence of a forcing term in the momentum equation, which leads to a non-zero correlation with the magnetic field. Finally, the application to energy convergence in solar wind turbulence is discussed.

**Key words:** magnetic fields – MHD – hydrodynamics – turbulence.

## 1 INTRODUCTION

The dynamo effect in astrophysical objects is often associated with the occurrence of helicity in them. In magnetohydrodynamics, there are several helicities that can be important. A particularly important one is the kinetic helicity, because its value is finite in rotating stratified bodies and can lead to an  $\alpha$  effect (Moffatt 1978; Parker 1979; Krause & Rädler 1980). Another important helicity is the magnetic helicity. Unlike the kinetic helicity, the magnetic helicity is conserved by the quadratic interactions, so its value can only change through resistive effects or through magnetic helicity fluxes (Brandenburg & Subramanian 2005). Such a conservation law is crucial to understanding the saturation behaviour of  $\alpha$  effect dynamos. This is because the  $\alpha$  effect tends to produce large-scale magnetic fields that are helical, but conservation of total magnetic helicity implies that there must be small-scale magnetic helicity of the opposite sign, so that the sum of small- and large-scale magnetic helicities is close to zero. This then leads to a resistively slow saturation phase in the non-linear regime (Brandenburg 2001). Mathematically, the consequence of magnetic helicity conservation can be described by the attenuation of the total  $\alpha$  effect by the addition of a term proportional to the magnetic helicity effect (Blackman & Brandenburg 2002; Field & Blackman 2002).

In a topological sense, magnetic helicity describes the linkage of magnetic flux tubes (Moffatt 1969), while the kinetic helicity char-

acterizes the linkage of vorticity tubes. However, there is yet another helicity, the cross-helicity, that describes the linkage of magnetic flux tubes with vortex tubes. This quantity is important because it too is conserved by the quadratic interactions, i.e. it can change only by visco-resistive effects or by cross-helicity fluxes. Moreover, the small-scale cross-helicity can itself lead to large-scale dynamo action (Yoshizawa 1990). Such a mechanism is quite different from the  $\alpha$  effect, because it corresponds to an inhomogeneous term in the dynamo equations and could therefore play the role of a turbulent battery term. Indeed, Brandenburg & Urpin (1998) showed that the battery term due to cross-helicity can facilitate large-scale dynamo action in young galaxies and hence could be responsible for the relatively strong magnetic fields observed in such galaxies at high redshifts.

In spite of several additional studies (Yoshizawa & Yokoi 1993; Yokoi 1996; Blackman & Chou 1997), large-scale dynamo action due to cross-helicity has not received much attention because this effect was never seen in simulations, nor was it found to be responsible for driving large-scale magnetic fields found therein. Such an effect would require that the small-scale magnetic field is systematically aligned with the flow, i.e. it is either mostly parallel or mostly antiparallel to the flow. Such circumstances are known to prevail in the solar wind, but here the field comes presumably directly from the Sun and would therefore not be produced by a dynamo.

In the present paper, we consider the so-called Archontis (2000) dynamo (see also Dorch & Archontis 2004; Cameron & Galloway 2006) which is driven by a forcing function that is based on the Arnold–Beltrami–Childress (or ABC) flow, but with the cosine

★E-mail: sur@iucaa.ernet.in (SS); brandenb@nordita.org (AB)

terms being omitted. This flow was first proposed by Galloway & Proctor (1992) to study fast dynamo action by calculating growth rates for the kinematic version of this flow. The ABC flow is helical and produces efficient dynamo action (Galloway & Frisch 1986). However, the omission of cosine terms renders the flow non-helical, so that there is no  $\alpha$  effect, but numerical studies (Dorch & Archontis 2004) have shown that such a dynamo produces magnetic fields that are either aligned or anti-aligned with the flow almost everywhere. This means that there is cross-helicity in the system, which can give rise to the Yoshizawa effect and produce large-scale dynamo action. Furthermore, owing to the conservation property of cross-helicity, such dynamos may be controlled by this effect and may also show slow saturation behaviour. It is therefore of interest to investigate whether the formulation for the slow saturation of  $\alpha$  effect dynamos carries over to the present case.

We begin by explaining first the simulations, discuss the features of the kinematic growth phase of the dynamo and then consider the slow saturation regime using a non-linear dynamical feedback formalism that is analogous to the dynamical quenching formalism for the  $\alpha$  effect. Next, we argue that the kinematic growth in such a dynamo is indeed due to the cross-helicity effect. We show that the estimated growth rate obtained from a simple model involving the induction and momentum equations along with the evolution equation for the small-scale cross-helicity can be brought in good agreement with our simulation results.

## 2 BASIC EQUATIONS

We consider here a model that is similar to that of Archontis (2000) and Dorch & Archontis (2004) who assumed a compressible gas with an energy equation included. However, in their model the temperature was kept approximately constant by applying a heating and cooling term. Here, we assume instead an isothermal equation of state, i.e. the pressure is given by  $p = \rho c_s^2$ , where  $\rho$  is the density and  $c_s$  is the isothermal sound speed. The evolution equations for the density  $\rho$ , velocity  $\mathbf{U}$  and magnetic vector potential  $\mathbf{A}$  are then

$$\frac{D \ln \rho}{Dt} = -\nabla \cdot \mathbf{U}, \quad (1)$$

$$\frac{D\mathbf{U}}{Dt} = -c_s^2 \nabla \ln \rho + \mathbf{F} + \frac{1}{\rho} [\mathbf{J} \times \mathbf{B} + \nabla \cdot (2\rho\nu\mathbf{S})], \quad (2)$$

$$\frac{\partial \mathbf{A}}{\partial t} = \mathbf{U} \times \mathbf{B} + \eta \nabla^2 \mathbf{A}, \quad (3)$$

where  $D/Dt = \partial/\partial t + \mathbf{U} \cdot \nabla$  is the advective derivative,  $\mathbf{B} = \nabla \times \mathbf{A}$  is the magnetic field,  $\mathbf{J} = \nabla \times \mathbf{B}/\mu_0$  is the current density,  $\mu_0$  is the vacuum permeability,  $\eta$  is the magnetic diffusivity, which is assumed constant,  $\nu$  is the kinematic viscosity,

$$S_{ij} = \frac{1}{2}(U_{i,j} + U_{j,i}) - \frac{1}{3}\delta_{ij} \nabla \cdot \mathbf{U} \quad (4)$$

is the traceless rate of strain tensor and

$$\mathbf{F} = F_0 (\sin k_0 z, \sin k_0 x, \sin k_0 y) \quad (5)$$

is the forcing function where  $F_0$  is an amplitude factor and  $k_0$  is a wavenumber.

For analytic considerations, we consider the flow to be incompressible, i.e.  $\nabla \cdot \mathbf{U} = 0$  and  $\rho = \rho_0 = \text{const}$ . While this simplifies the treatment significantly, it should be remembered that the differences between compressible and incompressible cases are not critical if the Mach number is small (Cameron & Galloway 2006). In the present paper, we consider cases where the Mach number is

around 0.03 (see below). In order to simplify the notation, we use units, where

$$k_0 = c_s = \rho_0 = \mu_0 = 1, \quad (6)$$

although in several places we shall keep these units for clarity.

The simulations have been performed using the `PENCIL` code.<sup>1</sup> Triply periodic boundary conditions are employed for all variables over a cubic domain of size  $L \times L \times L$ . As initial condition, we use zero velocity, constant density given by  $\rho = \rho_0$  and a spatially random vector potential of sufficiently low amplitude so as to obtain a clear initial exponential growth phase over several orders of magnitude before non-linear effects become important and lead to saturation of the magnetic field.

Our simulations are characterized by the values of the magnetic Reynolds and Prandtl numbers,

$$R_m = \frac{u_0}{\eta k_0} \quad \text{and} \quad P_m = \frac{\nu}{\eta}, \quad (7)$$

respectively. Here, we have defined  $u_0 = (F_0/k_0)^{1/2}$  as our reference velocity. Occasionally, we also use the visco-resistive Reynolds number,

$$R_\mu = \frac{u_0}{\mu k_0} = \frac{R_m}{1 + P_m}, \quad (8)$$

where  $\mu = \nu + \eta$ . Throughout this paper, we restrict ourselves to the case  $P_m = 1$ . The forcing amplitude is chosen such that the Mach number,  $\text{Ma} = u_0/c_s$ , is small (about 0.03), so the flow stays close to incompressible.

The flow is of course isotropic with respect to the three coordinate directions, so there is no preferred definition for the mean field in this case. Indeed, there are three equivalent definitions of two-dimensional averages ( $xy$ ,  $yz$  and  $xz$  averages). They all would lead to finite mean flows and mean magnetic fields. In the following, we consider mean fields defined by averaging over the  $x$  and  $y$  directions, i.e.

$$\overline{\mathbf{B}}(z, t) = \frac{1}{L^2} \int \mathbf{B} \, dx \, dy. \quad (9)$$

Throughout this paper, we focus on the case  $L = L_0$ , where we have defined  $L_0 = 2\pi/k_0$ . However, on one occasion we compare with the cases  $L = 2L_0$  and  $4L_0$ , where the domain is big enough to allow for a field configuration that is four times bigger than the wavelength of the sine waves. The residual,  $\mathbf{b} = \mathbf{B} - \overline{\mathbf{B}}$ , is normally referred to as the small-scale or fluctuating field, but in the present case such a characterization might be misleading, because such a field is quite regular and not actually fluctuating in the real sense of the word. Note in particular that the forcing function has a finite average, i.e.

$$\overline{\mathbf{F}}(z) = F_0 (\sin k_0 z, 0, 0), \quad (10)$$

so the residual is  $\mathbf{f} = F_0 (0, \sin k_0 x, \sin k_0 y)$ . It turns out that also  $\overline{\mathbf{U}}$  and  $\overline{\mathbf{B}}$  point mainly in the  $x$  direction. Throughout this paper, we denote the residuals by lower-case characters.

## 3 SIMULATION RESULTS

Dynamo action is possible once the value of  $R_m$  exceeds a certain critical value of around 3 (see Fig. 1). A similar curve was first shown by Galloway & Proctor (1992) for the case of a prescribed flow  $\mathbf{U} = u_0$ . For smaller values of  $R_m$ , the growth rate is negative while for larger values it levels off at a value comparable to  $u_0 k_0$ .

<sup>1</sup> <http://pencil-code.googlecode.com>

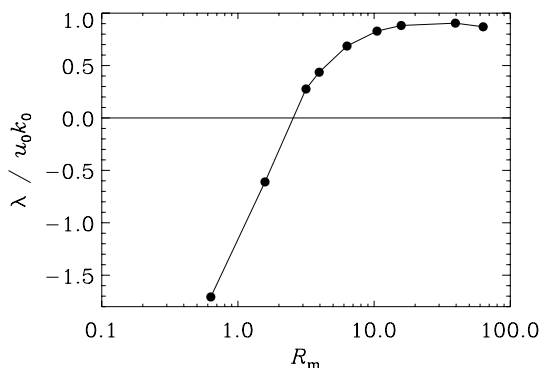


**Figure 1.** Dependence of the dynamo growth rate  $\lambda$  on  $R_m$ . Note that the critical value of  $R_m$  for dynamo action is around 3. For larger values of  $R_m$ , the growth rate levels off at a value around  $u_0 k_0$ .

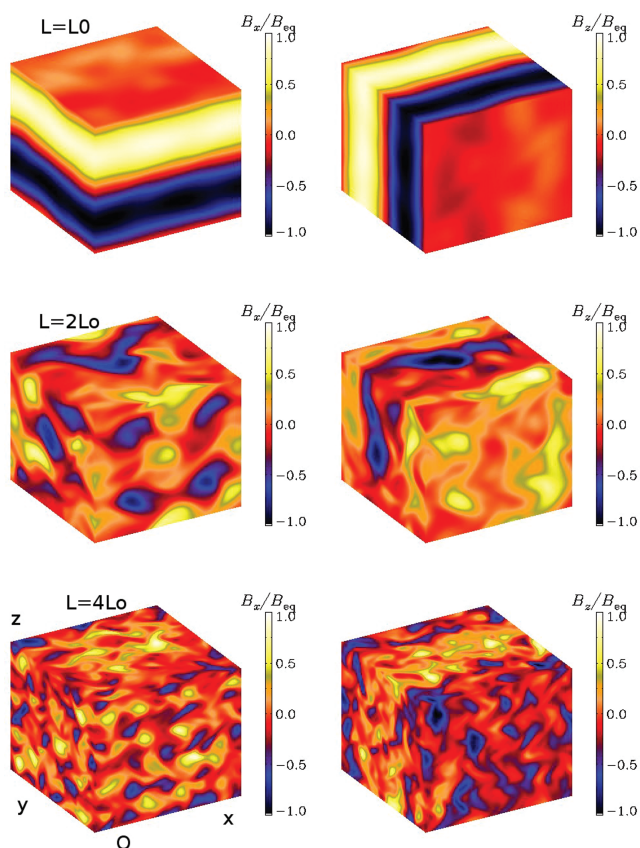


**Figure 2.** Visualization of  $B_x$  and  $B_z$  on the periphery of the domain in models with  $L/L_0 = 1$  (upper row), 2 (middle row) and 4 (lower row) for  $R_m = 13$ . In the case  $L = L_0$ , the magnetic field has a scale that is equal to that of the flow, but in the other cases the field breaks up into smaller-scale contributions with a modulation in the  $y$  direction on the scale of the domain. The coordinate directions are indicated in the lower-left panel and the origin is indicated by O.

One may expect the Archontis flow to be a small-scale dynamo, which means that the scale of the field would not exceed the scale of the flow,  $L_0$ . In order to check whether this flow can also generate fields on a scale larger than that of the flow we consider now also cases with  $L = 2L_0$  and  $4L_0$ . In Fig. 2, we compare visualizations of  $B_x$  and  $B_z$  for  $L/L_0 = 1, 2$  and  $4$ . In the case  $L = L_0$ , the magnetic field has a scale that is equal to that of the flow, but in the other cases the field breaks up into smaller-scale contributions

with a modulation in the  $y$  direction on the scale of the domain. In the latter case, the field on the scale of the domain is reminiscent of that found in helical turbulence (Brandenburg 2001), but it is less dominant and less persistent than for  $L = L_0$ . This is mainly explained by a strong reduction of net cross-helicity when the field breaks up into smaller-scale contributions. For these reasons, we focus in the remainder of this paper on the case  $L = L_0$ , which is perhaps the simplest case known to produce net cross-helicity.

Dynamos with  $L > L_0$  produce large-scale fields, but they are not as prominent and persistent as in the case of large-scale dynamos that are driven by kinetic helicity. This is mainly because in the simulations with larger domains the cross-helicity is strongly reduced once the magnetic field breaks up into smaller-scale fields.

In Fig. 3, we show the evolution of the mean magnetic field, mean velocity and the small-scale cross-helicity,  $h_c = \langle \mathbf{u} \cdot \mathbf{b} \rangle$ , for a run with  $R_m = 16$  in a logarithmic scale; see panel 1 and also the evolution of the magnetic energy compared to that of an  $\alpha^2$  dynamo on a linear scale in panel 2. Time is normalized with respect to the microscopic visco-resistive time-scale,  $(\mu k_0^2)^{-1}$ . Given that the initial magnetic field is spatially random, it is first smoothed by resistive effects, leading to a short period where the magnetic energy decreases. Exponential growth occurs after about half a visco-resistive time, and then turns into a slow saturation phase after about two visco-resistive times, which is best seen on a linear scale (lower panel of Fig. 3). However, the late saturation behaviour deviates from that of the  $\alpha^2$  dynamo, where the late evolution of the mean field is well described by a switch-on curve of the form

$$\overline{B}^2 \sim 1 - \exp(-\Delta t / \tau_\eta), \quad (11)$$

where  $\Delta t = t - t_s$  is the time after the end of the exponential growth phase at  $t = t_s$  and  $\tau_\eta = (2\eta k_1^2)^{-1}$  is the large-scale resistive time based on the wavenumber  $k_1$ , which would be equal to  $k_0$  in the present case.

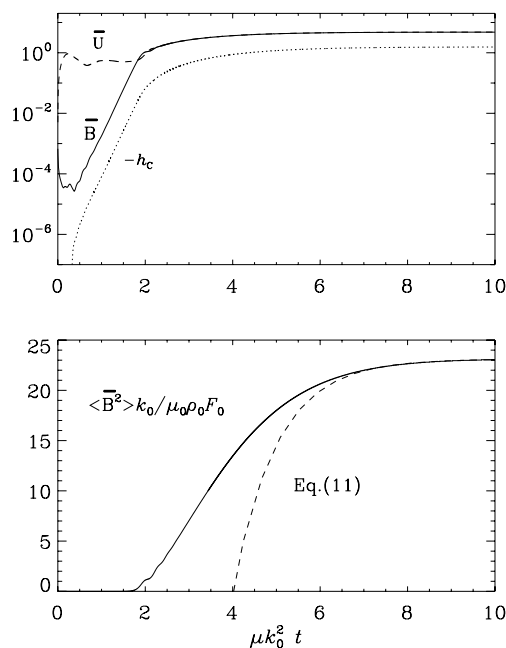


**Figure 3.** Saturation behaviour for a run with  $R_m = 16$ . The dotted line shows that the simple-minded helicity constraint formula does not describe the saturation of  $\overline{B}^2$  correctly. The labels  $\overline{U}$ ,  $\overline{B}$  and  $h_c$  denote  $(\overline{U}^2 k_0 / F_0)^{1/2}$ ,  $(\overline{B}^2 k_0 / \mu_0 \rho_0 F_0)^{1/2}$  and  $\langle \mathbf{u} \cdot \mathbf{b} \rangle (k_0 / F_0)^{1/2} (\mu_0 \rho_0)^{-1/4}$ .

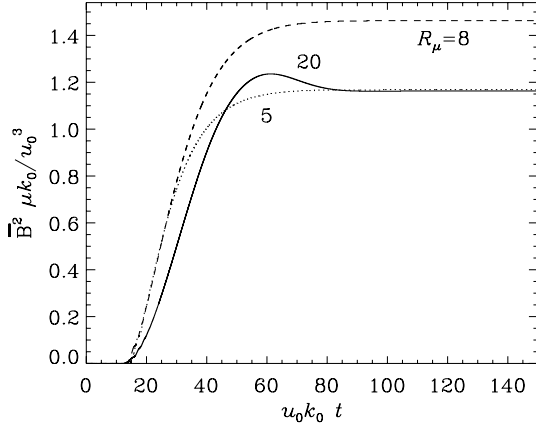


**Figure 4.** Comparison of the saturation behaviour for three different values of  $R_\mu$ .

In Fig. 4, we demonstrate that the saturation time is essentially independent of the value of  $R_\mu$ . Here, time is expressed in dynamical units by normalizing it in terms of the turnover time  $(u_0 k_0)^{-1}$ . The amplitude of the mean field increases mildly with  $R_\mu$ . A suitable non-dimensional representation of the mean field is the quantity  $\overline{B}^2 \mu k_0 / \mu_0 \rho_0 u_0^2$ . This number turns out to be of order unity and only weakly dependent on the value of  $R_\mu$  for values between 5 and 20.

In the three cases displayed in Fig. 4, we have verified that the choice of averaging is unimportant. In other words, the results for  $yz$  and  $xz$  averages agree with those for the  $xy$  averages shown in Fig. 4 within 0.1–0.5 per cent.

#### 4 TURBULENT MAGNETIC DIFFUSIVITY

In a number of circumstances, it has been possible to characterize the production of mean magnetic field in terms of  $\alpha$  effect and turbulent magnetic diffusivity. Here, ‘turbulent’ refers to the commonly used name for transport coefficients describing the evolution of mean fields rather than a distinction between turbulent and laminar flow properties. Both  $\alpha$  effect and turbulent magnetic diffusivity have been determined also for other laminar flows such as the Roberts flow (Brandenburg, Rädler & Schrunner 2008c). However, such a description may not be applicable in the present case because of the possible presence of the additional Yoshizawa effect. Ignoring this complication for a moment, we can determine the  $\alpha_{ij}$  and  $\eta_{ij}$  tensors in the relation

$$(\mathbf{u} \times \mathbf{b})_i = \alpha_{ij} \overline{B}_j - \eta_{ij} \overline{J}_j, \quad (12)$$

using the test-field method (Schrunner et al. 2005, 2007). In this approach, one solves an additional set of three-dimensional partial differential equations for vector fields  $\mathbf{b}^{pq}$ , where the labels  $p = 1, 2$  and  $q = 1, 2$  correspond to different pre-determined one-dimensional test fields  $\overline{\mathbf{B}}^{pq}$ . This leads to four vector equations for  $\mathbf{u} \times \mathbf{b}^{pq}$  that allow us to determine all components of  $\alpha_{ij}$  and  $\eta_{ij}$  as functions of  $z$  and  $t$ . Owing to homogeneity and stationarity, it makes sense to present their averages over  $z$  and  $t$ . The test-field method has been criticized by Cattaneo & Hughes (2009) on the grounds that the small-scale dynamo action would affect the results. However, for magnetic Reynolds numbers of up to about 100 the results of the test-field method have been proven to be consistent with results from direct simulations (Mitra et al. 2009).

The evolution equations for  $\mathbf{b}^{pq}$  are derived by subtracting the mean-field evolution equation from the evolution equation for  $\mathbf{B}$ . These equations are distinct from the original induction equation in

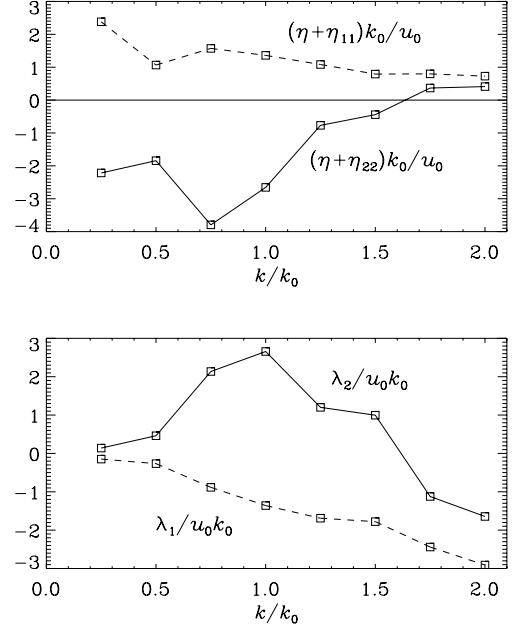


**Figure 5.** Dependence of the normalized diagonal components of the turbulent resistivity tensor for  $R_m = 6$  (upper panel) together with the corresponding growth rates (lower panel).

that the curl of the resulting mean electromotive force is subtracted. This method has been successfully applied to the kinematic case of weak magnetic fields in the presence of homogeneous turbulence either without shear (Brandenburg et al. 2008c; Sur, Brandenburg & Subramanian 2008) or with shear (Brandenburg 2005; Brandenburg et al. 2008a), as well as to the non-kinematic case with equipartition-strength dynamo-generated magnetic fields (Brandenburg et al. 2008b; Tilgner & Brandenburg 2008).

Using this method, it turns out that all components of  $\alpha_{ij}$  vanish within error bars, and that  $\eta_{ij}$  has only diagonal components. However, as shown in Fig. 5, the  $\eta_{22}$  component can be negative within a limited range of wavenumbers. (The fact that  $\eta_{11} \neq \eta_{22}$  is not a priori surprising, because both  $\overline{\mathbf{U}}$  and  $\overline{\mathbf{B}}$  have only components in the  $x$  direction.) One of the two growth rates,

$$\lambda_1 = -(\eta + \eta_{11})k_0^2, \quad \lambda_2 = -(\eta + \eta_{22})k_0^2, \quad (13)$$

is therefore positive. This suggests that there is the possibility of driving a dynamo by a negative turbulent resistivity effect (Zheligovsky, Podvigina & Frisch 2001; Urpin 2002). In such a case, it is important to determine the wavenumber where the growth rate is largest. In our case, this happens for  $k \approx k_1$  (see lower panel of Fig. 5).

In the following, we discard the possibility of dynamo activity driven through a negative turbulent resistivity effect, because the test-field method ignores the presence of the Yoshizawa effect. Thus, we argue that equation (12) is an *inadequate* ansatz that results in an apparent negative turbulent resistivity component. In the absence of a proper method for determining  $\eta_{ij}$ , we consider now a phenomenological description of the Yoshizawa effect using an isotropic turbulent resistivity,  $\eta_t$ .

#### 5 PHENOMENOLOGY

The slow saturation process found here is reminiscent of the slow saturation process found for the  $\alpha^2$  dynamo, where net magnetic helicity is being produced on a resistive time-scale. In the present

case, the magnetic helicity is essentially zero, but net cross-helicity is being produced. Owing to the conservation of cross-helicity, there is the possibility here too that full saturation requires a visco-resistive time-scale,  $\tau_\mu = (\mu k_f^2)^{-1}$ , where  $\mu = \nu + \eta$  and  $k_f$  is the wavenumber corresponding to the typical scale of  $\mathbf{u}$  and  $\mathbf{b}$ . In our case, these fields depend essentially only on the  $x$  and  $y$  directions, so  $k_f^2 = 2k_0^2$ . The form of this relation is not known, although it is already clear that it is not the same as in the case of the non-linear  $\alpha$  effect. Most importantly, the saturation time does not seem to depend sensitively on the value of  $R_\mu$  (Fig. 4). Moreover, owing to the presence of a forcing term in the momentum equation, the cross-helicity is not necessarily conserved in the limit  $\mu \rightarrow 0$ , but it may change. Indeed, under the assumption of incompressibility, the evolution of the cross-helicity per unit volume,  $\langle \mathbf{U} \cdot \mathbf{B} \rangle$ , is given by

$$\frac{d}{dt} \langle \mathbf{U} \cdot \mathbf{B} \rangle = \langle \mathbf{F} \cdot \mathbf{B} \rangle - \mu \langle \mathbf{W} \cdot \mathbf{J} \rangle. \quad (14)$$

Here, angular brackets denote volume averages and  $\mathbf{W} = \nabla \times \mathbf{U}$  is the vorticity. Note the presence of the forcing term that can lead to the production of net cross-helicity if the field has a component that is aligned with the forcing.

Next, we restrict ourselves to horizontal averages, denoted by an overbar, and consider first their evolution equations,

$$\frac{\partial}{\partial t} \bar{\mathbf{A}} = \bar{\mathbf{U}} \times \bar{\mathbf{B}} + \bar{\mathcal{E}} - \eta_t \bar{\mathbf{J}}, \quad (15)$$

$$\frac{\partial}{\partial t} \bar{\mathbf{U}} = \bar{\mathbf{U}} \times \bar{\mathbf{W}} + \bar{\mathbf{J}} \times \bar{\mathbf{B}} + \bar{\mathcal{F}} + \bar{\mathcal{F}} - \nu \bar{\mathbf{Q}}, \quad (16)$$

where  $\bar{\mathcal{E}} = \overline{\mathbf{u} \times \mathbf{b}}$  is the mean electromotive force due to the correlation of small-scale velocity and magnetic field correlations,  $\bar{\mathcal{F}} = \overline{\mathbf{u} \times \mathbf{w}} + \overline{\mathbf{j} \times \mathbf{b}}$  is the mean force due to advection and Lorentz force of small-scale contributions and  $\bar{\mathbf{Q}} = \nabla \times \bar{\mathbf{W}}$  is the curl of the vorticity. As discussed above, lower-case characters denote the residual or ‘fluctuating’ components, so, for example,  $\mathbf{w} = \mathbf{W} - \bar{\mathbf{W}}$  is the residual vorticity.

We note that the  $\bar{\mathbf{U}} \times \bar{\mathbf{W}}$  and  $\bar{\mathbf{J}} \times \bar{\mathbf{B}}$  terms will be of no significance, because for our one-dimensional  $z$ -dependent averages only the  $x$  and  $y$  components of  $\bar{\mathbf{A}}$  and  $\bar{\mathbf{U}}$  will be important for the evolution of the dynamo. We assume that  $\bar{\mathcal{E}}$  has only contributions from the Yoshizawa (1990) effect and from turbulent resistivity and that  $\bar{\mathcal{F}}$  has only a contribution from turbulent viscosity, i.e.

$$\bar{\mathcal{E}} = \Upsilon \bar{\mathbf{W}} - \eta_t \bar{\mathbf{J}}, \quad (17)$$

$$\bar{\mathcal{F}} = -\nu_t \bar{\mathbf{Q}}. \quad (18)$$

A simplified derivation of the Yoshizawa (1990) effect is given in Appendix A, which shows that

$$\Upsilon = \tau \overline{\mathbf{u} \cdot \mathbf{b}}. \quad (19)$$

We have chosen here the symbol  $\Upsilon$  instead of Yoshizawa’s original symbol  $\gamma$ , because  $\gamma$  is frequently used to describe the turbulent pumping velocity. Furthermore,  $\Upsilon$  looks similar to  $\gamma$  and it also reminds of the letter Y in Yoshizawa’s name.

In addition, there is also turbulent viscosity  $\nu_t = \frac{2}{15} \tau \overline{\mathbf{u}^2}$  and turbulent resistivity  $\eta_t = \frac{1}{3} \tau \overline{\mathbf{u}^2}$  (Kitchatinov, Rüdiger & Pipin 1994), although numerical simulations suggest  $\nu_t \approx \eta_t$  (Yousef, Brandenburg & Rüdiger 2003). Here,  $\tau$  is a typical time-scale that may be estimated in terms of the turnover time,  $\tau = (u_{\text{rms}} k_0)^{-1}$ , where  $u_{\text{rms}} = \langle \mathbf{u}^2 \rangle^{1/2}$ .

Inserting equations (17) and (18) into equations (15) and (16), we derive the following evolution equation for the cross-helicities

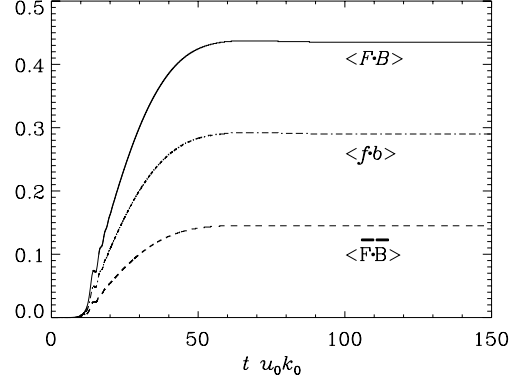


**Figure 6.** Plot of the force-magnetic field correlations for a run with  $R_m = 32$ .

of the mean and fluctuating fields:

$$\frac{d}{dt} \langle \bar{\mathbf{U}} \cdot \bar{\mathbf{B}} \rangle = \langle \bar{\mathbf{F}} \cdot \bar{\mathbf{B}} \rangle + \Upsilon \langle \bar{\mathbf{W}}^2 \rangle - \mu_T \langle \bar{\mathbf{W}} \cdot \bar{\mathbf{J}} \rangle, \quad (20)$$

$$\frac{d}{dt} \langle \mathbf{u} \cdot \mathbf{b} \rangle = \langle \mathbf{f} \cdot \mathbf{b} \rangle - \Upsilon \langle \bar{\mathbf{W}}^2 \rangle + \mu_t \langle \bar{\mathbf{W}} \cdot \bar{\mathbf{J}} \rangle - \mu \langle \mathbf{w} \cdot \mathbf{j} \rangle, \quad (21)$$

where  $\mu_t = \nu_t + \eta_t$  is the sum of turbulent viscosity and resistivity and  $\mu_T = \mu_t + \mu$  is the total (turbulent and microscopic) value. One can easily verify that the sum of equations (20) and (21) gives equation (14).

In the following, we shall use equation (21) to describe the evolution of  $\Upsilon$  fully in terms of mean-field quantities. This approach was recently pursued by Kandas (2007) for the more complete case where kinetic and magnetic helicities are also present. In equation (21), the term  $\langle \mathbf{u} \cdot \mathbf{b} \rangle$  is directly related to the mean-field quantity  $\Upsilon$ , and so is  $\langle \mathbf{w} \cdot \mathbf{j} \rangle = k_f^2 \langle \mathbf{u} \cdot \mathbf{b} \rangle$ . An exception is the correlation of the forcing term with  $\mathbf{b}$ , i.e. the term  $\langle \mathbf{f} \cdot \mathbf{b} \rangle$ . However, it turns out that for the Archontis flow considered here, each of the three terms,  $\langle F_i B_i \rangle$  for  $i = 1, 2$  and  $3$ , contributes equal amount, so  $\langle \bar{\mathbf{F}} \cdot \bar{\mathbf{B}} \rangle = \frac{1}{3} \langle \mathbf{F} \cdot \mathbf{B} \rangle$  and  $\langle \mathbf{f} \cdot \mathbf{b} \rangle = \frac{2}{3} \langle \mathbf{F} \cdot \mathbf{B} \rangle$ , so that we can express

$$\langle \mathbf{f} \cdot \mathbf{b} \rangle = 2 \langle \bar{\mathbf{F}} \cdot \bar{\mathbf{B}} \rangle \quad (22)$$

purely in terms of mean-field quantities. The validity of these relations can be seen in Fig. 6, where we plot the aforementioned correlations for a run with  $R_m = 32$ .

With these preparations, we can write down an evolution equation for  $\Upsilon$ ,

$$\frac{d\Upsilon}{dt} = 2\tau \langle \bar{\mathbf{F}} \cdot \bar{\mathbf{B}} \rangle - \tau \Upsilon \bar{\mathbf{W}}^2 + \mu_t \tau \langle \bar{\mathbf{J}} \cdot \bar{\mathbf{W}} \rangle - \tilde{R}_\mu^{-1} \frac{\Upsilon}{\tau}, \quad (23)$$

where we have defined a modified visco-resistive Reynolds number

$$\tilde{R}_\mu = (\mu k_f^2 \tau)^{-1}. \quad (24)$$

Note that it is related to  $R_\mu$  via

$$\tilde{R}_\mu = (k_f/k_0)^2 (u_{\text{rms}}/u_0) R_\mu. \quad (25)$$

Analogous to the magnetic case, we can write this equation as a quenching formula by keeping the time derivative as an implicit term,

$$\Upsilon = \tilde{R}_\mu \frac{2\tau^2 \langle \bar{\mathbf{F}} \cdot \bar{\mathbf{B}} \rangle + \tau^2 \mu_t \langle \bar{\mathbf{W}} \cdot \bar{\mathbf{J}} \rangle - \tau d\Upsilon/dt}{1 + \tilde{R}_\mu \langle \bar{\mathbf{W}}^2 \rangle \tau^2}. \quad (26)$$

These equations show that the generation of large-scale magnetic field by the  $\Upsilon$  term produces  $\langle \bar{\mathbf{U}} \cdot \bar{\mathbf{B}} \rangle$  of the same sign as that of

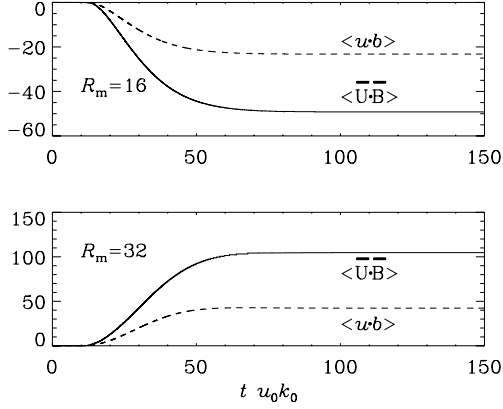


**Figure 7.** Saturation behaviour of large- and small-scale cross-helicities for two different values of  $R_m$ .

$\Upsilon (= \tau \overline{\mathbf{u}} \cdot \overline{\mathbf{b}})$ . This is also seen in the simulations, where  $\langle \overline{\mathbf{U}} \cdot \overline{\mathbf{B}} \rangle$  and  $\langle \mathbf{u} \cdot \mathbf{b} \rangle$  do indeed have identical signs for the same  $R_m$ , but could individually, depending on initial conditions, have different signs; see Fig. 7 for two cases with different  $R_m$  values. However, this sign property is a major difference to the case of the  $\alpha^2$  dynamo where  $\langle \overline{\mathbf{A}} \cdot \overline{\mathbf{B}} \rangle$  and  $\langle \mathbf{a} \cdot \mathbf{b} \rangle$  have opposite signs. The reason for this lies in the absence of a  $\Upsilon$  term that is independent of  $\overline{\mathbf{u}} \cdot \overline{\mathbf{b}}$ , i.e. there is only the term  $\Upsilon = \tau \overline{\mathbf{u}} \cdot \overline{\mathbf{b}}$ . By contrast, the  $\alpha$  effect has also a contribution from kinetic helicity that is independent of magnetic helicity, i.e.  $\alpha = \frac{1}{3} \tau \overline{\mathbf{j}} \cdot \overline{\mathbf{b}} - \frac{1}{3} \tau \overline{\boldsymbol{\omega}} \cdot \overline{\mathbf{u}}$ .

It is instructive to inspect this difference by comparing equation (26) with the analogous equation for  $\alpha$  quenching. Written in implicit form (see e.g. Brandenburg 2008), and ignoring magnetic helicity fluxes, this equation takes the form

$$\alpha = \frac{\alpha_0 + R_m (\eta_t \langle \overline{\mathbf{J}} \cdot \overline{\mathbf{B}} \rangle / B_{\text{eq}}^2 - \tau d\alpha/dt)}{1 + R_m \langle \overline{\mathbf{B}}^2 \rangle / B_{\text{eq}}^2}, \quad (27)$$

where  $B_{\text{eq}} = \langle \rho \mathbf{u}^2 \rangle^{1/2}$  is the equipartition field strength and  $\alpha_0$  is the kinematic  $\alpha$  effect, i.e. the term proportional to  $\overline{\boldsymbol{\omega}} \cdot \overline{\mathbf{u}}$ , which is the crucial term that has no correspondence with equation (26). Another difference is the presence of the forcing term in equation (26). Apart from that, the two equations are quite analogous, i.e.  $\tilde{R}_\mu$  is replaced by  $R_m$ ,  $\mu_t$  is replaced by  $\eta_t$ ,  $\Upsilon$  is replaced by  $\alpha$ ,  $\tau^2$  is replaced by  $B_{\text{eq}}^{-2}$  and  $\overline{\mathbf{W}}$  is replaced by  $\overline{\mathbf{B}}$ .

## 6 KINEMATIC GROWTH PHASE

The equations discussed above were originally motivated by trying to understand the late non-linear stage of the dynamo. However, as we see from equation (26),  $\Upsilon$  itself has terms proportional to the mean field, suggesting that  $\Upsilon$  should increase with the mean magnetic field. This is indeed the case during the kinematic stage; see the dotted line in the upper panel of Fig. 3. This suggests that the  $\Upsilon$  term might also be responsible for the kinematic exponential growth of the dynamo. In order to identify the relative importance of this mechanism compared with the negative magnetic diffusivity effect discussed at the end of Section 3, we investigate a simple model based on the induction and momentum equations along with the evolution equation for the small-scale cross-helicity. The  $z$ -dependent averaging procedure for the mean magnetic and velocity fields then implies,

$$\frac{\partial \overline{\mathbf{U}}}{\partial t} = \overline{\mathbf{F}} - \nu_T \overline{\mathbf{Q}}, \quad (28)$$

$$\frac{\partial \overline{\mathbf{B}}}{\partial t} = \nabla \times (\Upsilon \overline{\mathbf{W}} - \eta_T \overline{\mathbf{J}}), \quad (29)$$

where  $\nu_T = \nu_t + \nu$  and  $\eta_T = \eta_t + \eta$ . We write equations (28) and (29) along with equation (23) in the form

$$\dot{\mathbf{U}} = \mathbf{F}_0 - \nu_T k_0^2 \mathbf{U}, \quad (30)$$

$$\dot{\mathbf{B}} = \Upsilon k_0^2 \mathbf{U} - \eta_T k_0^2 \mathbf{B}, \quad (31)$$

$$\dot{\Upsilon} = 2\tau F_0 \mathbf{B} + \tau k_0^2 U (\mu_t \mathbf{B} - \Upsilon \mathbf{U}) - \tilde{R}_\mu^{-1} \tau^{-1} \Upsilon, \quad (32)$$

where the dots denote a time derivative and double  $z$  derivatives have been replaced by a multiplication with  $-k_0^2$ . During the early kinematic phase, the mean velocity is approximately constant. Simulation results for a run with  $R_m = 32$ , then yield  $\tilde{U} = U/u_0 \approx 0.6$ . Applying therefore equation (30) to the steady state gives  $\nu_T = F_0/k_0^2 U$ , i.e.  $\nu_T = 1.7u_0/k_0$ .

The early exponential growth of both  $\mathbf{B}$  and  $\Upsilon$  is governed by just the first terms on the RHS of equations (31) and (32), i.e.

$$\frac{d}{dt} \begin{pmatrix} \mathbf{B} \\ \Upsilon \end{pmatrix} = \begin{pmatrix} 0 & k_0^2 U \\ 2\tau F_0 & 0 \end{pmatrix}. \quad (33)$$

This assumes that the  $\eta_T$  term in equation (31) is negligible. Therefore, the expected maximal growth rate for the Yoshizawa effect is

$$\lambda_\Upsilon = \pm \sqrt{2F_0 \tau k_0^2 U}. \quad (34)$$

Here, we may estimate  $\tau$  in terms of the turnover time,  $\tau = (u_{\text{rms}} k_0)^{-1}$ . Our dimensionless turnover time,  $u_0/u_{\text{rms}}$ , is then about 0.4, so the dimensionless growth rate is

$$\frac{\lambda_\Upsilon}{u_0 k_0} = \pm \sqrt{2\tilde{\tau} \tilde{U}}. \quad (35)$$

This amounts to about 0.7, which is in good agreement with the simulation data. This suggests that the Yoshizawa effect may indeed be responsible for driving the dynamo in the kinematic stage.

This simple model does not describe the non-linear saturation process. So, if one wanted to model this, one would need to assume some ad hoc quenching prescriptions for various quantities such as  $\nu_t$ ,  $\eta_t$  and  $\tau$ . This is in stark contrast to the case of the  $\alpha^2$  dynamo where equation (27) describes both the kinematic growth and the slow saturation phase quite accurately in the case of periodic boundary conditions (Blackman & Brandenburg 2002; Field & Blackman 2002).

## 7 CONCLUSIONS

We considered here the Archontis flow, which is a generalization of the ABC flow. Such a flow was thought to be a small-scale dynamo capable of generating magnetic fields at most on the scale of the flow. However, this flow tends to produce net cross-helicity, which can lead to a mean-field dynamo effect proposed originally by Yoshizawa (1990). Direct numerical simulations of such flows performed with bigger box size show the presence of magnetic fields on scales larger than the scale of the box (Fig. 2). This is reminiscent of large-scale dynamos driven by kinetic helicity, where the resulting field is however much more prominent or persistent.

The strongest cross-helicity production is found when the scale of the domain coincides with that of the flow. In that case, dynamo action is possible once  $R_m$  exceeds a certain critical value which in our units turns out to be  $R_m \simeq 3$ . The present work has shown that the kinematic phase of the Archontis dynamo can be modelled in

terms of the Yoshizawa effect. The sign of the cross-helicity depends on initial conditions, so either sign is possible for one and the same flow field. Simple phenomenological considerations support the idea that the Yoshizawa effect can be expressed in terms of the mean field alone; see equation (26). This expression looks similar to the dynamical quenching formula for the  $\alpha$  effect under the constraint of magnetic helicity conservation. However, this expression does not actually describe quenching, but growth. So, contrary to our initial expectation, this mechanism is not constant in time and so it does not correspond to a battery with linear growth, as was assumed by Brandenburg & Urpin (1998). Instead, it leads to exponential growth. At the end of the exponential growth phase, the dynamo shows a characteristic saturation behaviour that is reminiscent of  $\alpha$  effect dynamos that are controlled by resistive magnetic helicity evolution. In the present case, the conservation of cross-helicity was initially thought to be responsible for this prolonged saturation behaviour, but it turns out that the presence of a forcing term in the momentum equation can lead to a production of net cross-helicity even in the ideal limit.

It has long been speculated that the Yoshizawa effect could be relevant in accretion discs and galaxies where differential rotation is strong (Yokoi 1996). However, it turns out that, unlike  $\alpha$  effect dynamos that normally have a given kinematic value of  $\alpha$ , the  $\Upsilon$  term cannot be calculated a priori, but it itself depends on the mean field. The end result is again reminiscent of the  $\alpha$  effect in that both  $\Upsilon \overline{\mathbf{W}}$  as well as  $\alpha \overline{\mathbf{B}}$  are linear in  $\overline{\mathbf{B}}$  during the kinematic growth phase. However, the results of the test-field method show clearly that there is no  $\alpha$  effect in that case. Indeed, the mean electromotive force has no component along the mean magnetic field, confirming that there is no  $\alpha$  effect. There is also no shear-current (or  $\overline{\mathbf{W}} \times \overline{\mathbf{J}}$ ) effect (Rogachevskii & Kleeorin 2003, 2004), because the off-diagonal components of  $\eta_{ij}$  were found to be zero within error bars (Section 4). This supports the idea that the growth of the magnetic field is here indeed the result of the Yoshizawa effect. Although the  $\eta_{22}$  component is found to be negative when ignoring the Yoshizawa effect, it is argued that this result is an artefact of using an inadequate ansatz for the mean electromotive force.

Obviously, the flow considered here is relatively simple and hardly of direct astrophysical relevance. However, it has been suggested that dynamos with field-aligned flows might be particularly efficient in generating magnetic fields in the solar tachocline (Galloway 2008). If those ideas can be substantiated, it would be interesting to see whether the phenomenological description developed in the present paper carries over also to other cases such as this tachocline model.

Another possible avenue for future research would be the study of fully turbulent dynamos in the presence of cross-helicity. An example of this was shown in Fig. 2, where the flow was driven by the Archontis forcing function, but on a scale that is smaller than that of the computational domain. Those dynamos produce large-scale fields, but they are not as prominent and persistent as in the case of large-scale dynamos that are driven by kinetic helicity. This is mainly because in the simulations with larger domains the cross-helicity is strongly reduced once the magnetic field breaks up into smaller-scale fields.

As mentioned in the introduction, the solar wind is one of the few examples where the turbulence is believed to have net cross-helicity, but with opposite signs in the two hemispheres. Although the solar wind is not normally thought to harbour dynamos, there is the problem of an unexplained contribution to energy deposition away from the source. It would therefore be worthwhile exploring

the role of the Yoshizawa effect in the conversion of energy in solar wind turbulence.

## ACKNOWLEDGMENTS

We thank the organizers of the program ‘Magnetohydrodynamics of Stellar Interiors’ at the Isaac Newton Institute in Cambridge (UK) for creating a stimulating environment that led to the present work, and Robert Cameron and David Galloway for inspiring discussions. SS thanks Nordita for hospitality during the course of this work and the Council of Scientific and Industrial Research, India for providing financial support. We acknowledge the use of the HPC facility (Cetus cluster) at IUCAA, the National Supercomputer Centre in Linköping and the Center for Parallel Computers at the Royal Institute of Technology in Sweden. This work was supported in part by the Swedish Research Council, grant 621-2007-4064, and the European Research Council under the AstroDyn Research Project 227952.

## REFERENCES

- Archontis V., 2000, PhD thesis, Univ. Copenhagen  
 Blackman E. G., Brandenburg A., 2002, *ApJ*, 579, 359  
 Blackman E. G., Chou T., 1997, *ApJ*, 489, L95  
 Blackman E. G., Field G. B., 2002, *Phys. Rev. Lett.*, 89, 265007  
 Brandenburg A., 2001, *ApJ*, 550, 824  
 Brandenburg A., 2005, *Astron. Nachr.*, 326, 787  
 Brandenburg A., 2008, *Astron. Nachr.*, 329, 725  
 Brandenburg A., Subramanian K., 2005, *Phys. Rep.*, 417, 1  
 Brandenburg A., Urpin V., 1998, *A&A*, 332, L41  
 Brandenburg A., Rädler K.-H., Rheinhardt M., Käpylä P. J., 2008a, *ApJ*, 676, 740  
 Brandenburg A., Rädler K.-H., Rheinhardt M., Subramanian K., 2008b, *ApJ*, 687, L49  
 Brandenburg A., Rädler K.-H., Schrunner M., 2008c, *A&A*, 482, 739  
 Cameron R., Galloway D., 2006, *MNRAS*, 365, 735  
 Cattaneo F., Hughes D. W., 2009, *MNRAS*, 395, L48  
 Dorch S. B. F., Archontis V., 2004, *Solar Phys.*, 224, 171  
 Field G. B., Blackman E. G., 2002, *ApJ*, 572, 685  
 Galloway D. J., 2008, ‘A Strong-Field Dynamo in the Solar Tachocline’, online talk given on 15 July 2008 at the Kavli Institute for Theoretical Physics in Santa Barbara ([http://online.kitp.ucsb.edu/online/dynamo\\_c08/galloway](http://online.kitp.ucsb.edu/online/dynamo_c08/galloway))  
 Galloway D., Frisch U., 1986, *Geophys. Astrophys. Fluid Dyn.*, 36, 53  
 Galloway D. J., Proctor M. R. E., 1992, *Nat*, 356, 691  
 Kandus A., 2007, *MNRAS*, 378, 1356  
 Kitchatinov L. L., Rüdiger G., Pipin V. V., 1994, *Astron. Nachr.*, 315, 157  
 Krause F., Rädler K.-H., 1980, *Mean-field Magnetohydrodynamics and Dynamo Theory*, Pergamon Press, Oxford  
 Mitra D., Käpylä P. J., Tavakol R., Brandenburg A., 2009, *A&A*, 495, 1  
 Moffatt H. K., 1969, *J. Fluid Mech.*, 35, 117  
 Moffatt H. K., 1978, *Magnetic Field Generation in Electrically Conducting Fluids*, Cambridge Univ. Press, Cambridge  
 Parker E. N., 1979, *Cosmical Magnetic Fields*, Clarendon Press, Oxford  
 Rogachevskii I., Kleeorin N., 2003, *Phys. Rev. E*, 68, 036301  
 Rogachevskii I., Kleeorin N., 2004, *Phys. Rev. E*, 70, 046310  
 Schrunner M., Rädler K.-H., Schmitt D., Rheinhardt M., Christensen U., 2005, *Astron. Nachr.*, 326, 245  
 Schrunner M., Rädler K.-H., Schmitt D., Rheinhardt M., Christensen U., 2007, *Geophys. Astrophys. Fluid Dyn.*, 101, 81  
 Sur S., Brandenburg A., Subramanian K., 2008, *MNRAS*, 385, L15  
 Tilgner A., Brandenburg A., 2008, *MNRAS*, 391, 1477  
 Urpin V., 2002, *Phys. Rev. E*, 68, 036301  
 Yokoi N., 1996, *A&A*, 311, 731  
 Yoshizawa A., 1990, *Phys. Fluids B*, 2, 1589  
 Yoshizawa A., Yokoi N., 1993, *ApJ*, 407, 540

Yousef T. A., Brandenburg A., Rüdiger G., 2003, A&A, 411, 321  
 Zheligovsky V. A., Podvigina O. M., Frisch U., 2001, Geophys. Astrophys. Fluid Dyn., 95, 227

## APPENDIX A: CROSS-HELICITY EFFECT

We present here a simplified derivation of equation (19) using the minimal  $\tau$  approximation (Blackman & Field 2002). We use the linearized evolution equations for the fluctuations  $\mathbf{b}$  and  $\mathbf{u}$  and calculate

$$\partial \overline{\mathcal{E}} / \partial t = \overline{\mathbf{u} \times \dot{\mathbf{b}}} + \overline{\dot{\mathbf{u}} \times \mathbf{b}}. \quad (\text{A1})$$

In order to highlight the essence of the Yoshizawa (1990) term, we isolate from the very beginning the terms that are proportional to the mean vorticity. Thus, we consider in the evolution equations of  $\dot{\mathbf{b}}$  and  $\dot{\mathbf{u}}$  only those terms that contribute to terms proportional to  $\overline{\mathbf{W}}$  and write

$$\dot{\mathbf{b}} = +\mathbf{b} \cdot \nabla \overline{\mathbf{U}} + \dots = -\frac{1}{2} \mathbf{b} \times \overline{\mathbf{W}} + \dots, \quad (\text{A2})$$

$$\dot{\mathbf{u}} = -\mathbf{u} \cdot \nabla \overline{\mathbf{U}} + \dots = +\frac{1}{2} \mathbf{u} \times \overline{\mathbf{W}} + \dots, \quad (\text{A3})$$

where we have included only the antisymmetric contribution to  $\nabla \overline{\mathbf{U}}$  that leads to terms with  $\overline{\mathbf{W}}$ , i.e.  $\overline{U}_{i,j} = -\frac{1}{2} \epsilon_{ijk} \overline{W}_k$  + the symmetric

part, where a comma denotes a partial derivative. Next, we calculate  $\partial \overline{\mathcal{E}} / \partial t$  and include only terms proportional to  $\mathbf{u} \cdot \mathbf{b}$  by assuming  $u_i b_j = \frac{1}{3} \delta_{ij} \mathbf{u} \cdot \mathbf{b}$  + terms proportional to  $\mathbf{u} \times \mathbf{b}$ , but those would later not contribute to the component of  $\overline{\mathcal{E}}$  that is parallel to  $\overline{\mathbf{W}}$ . In this way, we obtain from  $\overline{\mathbf{u} \times \dot{\mathbf{b}}}$  and  $\overline{\dot{\mathbf{u}} \times \mathbf{b}}$  each the term  $\frac{1}{3} \overline{\mathbf{u} \cdot \mathbf{b}}$ , so

$$\partial \overline{\mathcal{E}} / \partial t = \frac{2}{3} \overline{\mathbf{u} \cdot \mathbf{b} \overline{\mathbf{W}}} + \dots - \text{triple correlations}. \quad (\text{A4})$$

In the spirit of the minimal  $\tau$  approximation, we approximate the triple correlations by a quadratic correlation in the form of a damping term, i.e. we assume that the triple correlations are equal to  $\overline{\mathcal{E}} / \tau$ . Finally, assuming stationarity, we drop the time derivative and obtain  $\overline{\mathcal{E}} = \frac{2}{3} \tau \overline{\mathbf{u} \cdot \mathbf{b} \overline{\mathbf{W}}}$ .

In an alternative derivation, one can write  $\mathbf{U} \cdot \nabla \mathbf{U} = \mathbf{U} \times \mathbf{W} - \frac{1}{2} \nabla U^2$  and subsume the gradient term in a generalized pressure term. Splitting  $\mathbf{U} \times \mathbf{W}$  into mean and fluctuating part yields then directly a term  $\mathbf{u} \times \overline{\mathbf{W}}$  without the 1/2 factor. The final result is then

$$\overline{\mathcal{E}} = \tau \overline{\mathbf{u} \cdot \mathbf{b} \overline{\mathbf{W}}}, \quad (\text{A5})$$

which is also the expression used here.

This paper has been typeset from a  $\text{\TeX}/\text{\LaTeX}$  file prepared by the author.